Magnetism and Electronic Structure of the (Pentamethylcyclopentadienyl)dichlororuthenium Dimers†

Ulrich Koelle,‡ Heiko Lueken,*,‡ Klaus Handrick,‡ Helmut Schilder,§ Jeremy K. Burdett,⊥ and Scarlett Balleza⊥

Institut für Anorganische Chemie, Rheinisch-Westfälische Technische Hochschule Aachen, Prof.-Pirlet-Strasse 1, D-52056 Aachen, FRG, Fachbereich Chemieingenieurwesen, Fachhochschule Aachen, Worringer Weg, D-52074 Aachen, FRG, and Department of Chemistry and the James Franck Institute, University of Chicago, Chicago, Illinois 60637

Received May 22, 1995[⊗]

The unit cell of the binuclear Ru(III) $4d^5$ (low spin, $S = {}^1/_2$) compound $[\{C_5(CH_3)_5\}Ru(\mu\text{-}Cl)Cl]_2$ contains two isomers **a** and **b** which differ distinctly in the Ru–Ru separation (2.93 Å (**a**), 3.75 Å (**b**)) and in the Ru–Cl–Ru bridge angle (76° (**a**), 100° (**b**)). Magnetic susceptibilities have been determined in the temperature range 3 to 295 K in order to assess the intramolecular spin couplings. Isomer **a** shows a comparatively strong intramolecular antiferromagnetism (singlet–triplet splitting ≥ 760 cm^{-1}), whereas in **b** a weak ferromagnetic coupling (triplet–singlet splitting ≈ 24 cm^{-1}) via the chlorine bridge is deduced. Extended Hückel calculations provide a qualitative explanation for the observed geometries and spin states of the two isomers. The electronic picture in these $t_{2g}{}^5t_{2g}{}^5$ compounds is very similar to that in the $e_g{}^3e_g{}^3$ copper dimers. Orbital crossing as a function of bridging angle leads to a change in spin state. The change in bonding character of the occupied orbitals allows an understanding of the bond length differences seen in the two isomers.

Introduction

Binuclear transition metal complexes with paramagnetic centers bridged by halogens or oxygen or nitrogen functions are interesting not only as versatile starting materials for the synthesis of monomeric coordination compounds but also for the study of metal–metal interactions.[1,2] Organometallic halide (X) bridged dimers $[L_RM(\mu\text{-}X)X_n]_2$ are known with π ligands L_R like arene, cyclopentadienyl, etc., and metals M ranging from titanium to platinum in the transition series.[3] Among them Cp^*RuCl_2 ($Cp^* \equiv \eta^5\text{-}C_5(CH_3)_5$) is a widely used reagent for the preparation of Cp*Ru complexes.

X-ray crystallography has disclosed a dimeric structure for Cp^*RuCl_2 [4] instead of a polymeric one, as is generally accepted in the literature.[5,6] An intriguing feature of the crystal structure of $[Cp^*Ru(\mu\text{-}Cl)Cl]_2$ (**1**) is the existence of two isomeric forms in the unit cell (ratio 1:1), both of them dimers with Ru(III) d^5 low-spin centers ($S = {}^1/_2$) but with distinctly different Ru–Ru separations of 2.93 and 3.75 Å and geometries of the bridging atoms (dimeric species **1a** and **1b** respectively; see Figure 1 and Table 1). This fortuitous finding offers an unique opportunity for a detailed study of the variation of intramolecular spin–spin coupling produced exclusively by alteration in geometry. Obviously the "deformational isomerism" in the crystals of **1** marks the transition from a binuclear system with a direct metal–metal bond to a system without bonding interaction between the metals.[7] Solid state ^{1}H and ^{13}C NMR shifts[8] indicate a diamagnetic dimer with sufficiently strong antiferromagnetically coupled Ru(III) centers (obviously molecule **1a** with the short Ru–Ru separation), along with a paramagnetic species (molecule **1b**). Temperature dependent ^{1}H NMR shifts in solution can be interpreted in terms of a rapid equilibrium of the two isomers.[4]

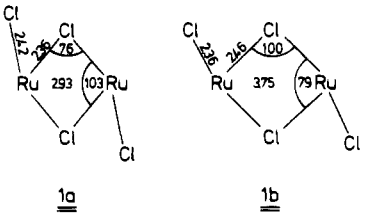

Figure 1. Ru–Cl bond lengths and Ru–Cl–Ru bond angles of **1a** and **1b**.

Table 1. Pertinent Bond Lengths and Angles in the Binuclear Compounds $[Cp^*RuX_2]_2$ (X = Cl(**1**), Br(**3**)) and $[Cp'RuCl_2]_2$ (**2**) (Bond Distances, Å; Angles, deg[4,c])

	1a	**1b**	**2**	**3**
Ru–Ru[a]	2.930(1)	3.752(1)	2.9256(3)	3.098(2)
Ru–X_T[b]	2.418(2)	2.365(2)	2.4147(6)	2.543(2)
Ru–X_B[c]	2.366(1)	2.445(1)	2.3619(6)	2.479(2)
Ru–X_B–Ru	76.50(4)	100.24(5)	76.53(2)	76.25
X_B–Ru–X_B'	103.50(4)	79.76(5)	103.47(2)	102.76
X_T–Ru–X_B[c]	89.99(6)	91.50(6)	89.56(2)	90.30

[a] Next but one Ru(**b**)–Ru(**b**) distance: 7.925 Å. [b] X_T, terminal halogen atom; X_B, bridging halogen atom. [c] Mean value.

† Dedicated to Professor Dr. P. Paetzold on the occasion of his 60th birthday.

‡ Rheinisch-Westfälische Technische Hochschule Aachen.

§ Fachhochschule Aachen.

⊥ University of Chicago.

⊗ Abstract published in *Advance ACS Abstracts,* November 1, 1995.

(1) Cotton, F. A. *Polyhedron* **1987**, *6*, 667.
(2) Willett, R. D., Gatteschi, D., Kahn, O., Eds. *Magneto-Structural Correlations in Exchange Coupled Systems*; NATO ASI Series, Series C, Vol. 140; Reidel: Dordrecht, Holland, 1985.
(3) Poli, R. *Chem. Rev.* **1991**, *91*, 509.
(4) Koelle, U.; Kossakowski, J.; Klaff, N.; Wesemann, L.; Englert, U.; Herberich, G. E. *Angew. Chem., Int. Ed. Engl.* **1991**, *30*, 690.
(5) Don Tilley, T.; Grubbs, R. H.; Bercaw, J. E. *Organometallics* **1984**, *3*, 274.
(6) Oshima, N.; Suzuki, H.; Moro-oka, Y. *Chem. Lett.* **1984**, 1161.
(7) The Ru–Ru distance in **1a** is at the long end of a Ru–Ru single bond (2.94 Å in $[Me_3SnRu(CO)_4]_2$: Bonny, A. *Coord. Chem. Rev.* **1978**, *25*, 229) but has also been observed in binuclear complexes lacking a direct Ru–Ru interaction (Koelle, U.; Kossakowski, J.; Boese, R. *J. Organomet. Chem.* **1989**, *378*, 449).
(8) Benn, R.; Grondey, H.; Koelle, U. *J. Magn. Reson.* **1990**, 89, 375.

0020-1669/95/1334-6273$09.00/0

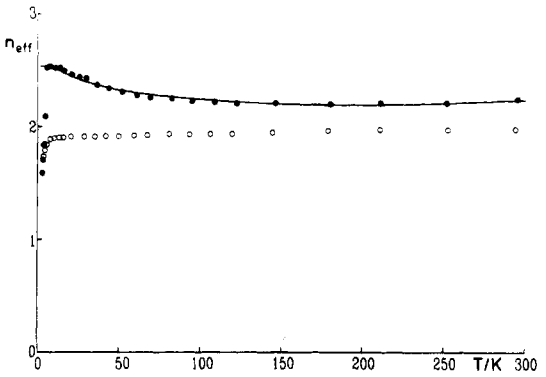

Figure 2. $n_{eff}-T$ diagrams of **1** (●) and **4** (○). Notice that n_{eff} in the case of **1** refers to two metal centers.

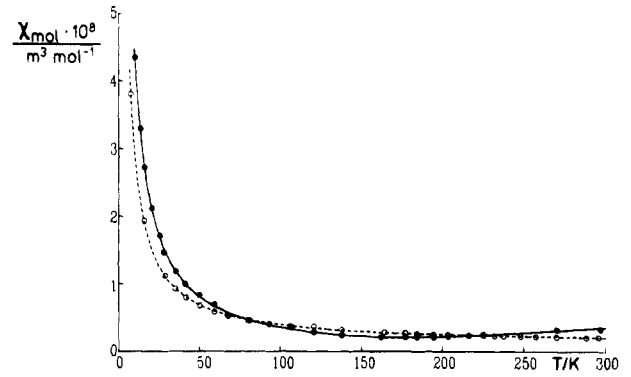

Figure 3. $\chi-T$ diagrams of **2** (●) and **3** (○).

In order to corroborate these conclusions and provide a deeper insight into the intramolecular spin couplings, the magnetic susceptibility of **1** has been determined. In addition, the magnetic and EPR behavior of several reference compounds have been investigated: (i) the magnetic susceptibility of $[Cp'Ru(\mu\text{-}Cl)Cl]_2$ (**2**) (Cp′ ≡ η^5-$C_5(CH_3)_4(C_2H_5)$) and $[Cp^*Ru(\mu\text{-}Br)Br]_2$ (**3**), consisting of molecules in the solid with geometry corresponding to isomer **1a** (Ru−Ru = 2.93 Å (**2**), 3.10 Å (**3**)[4]); (ii) the magnetic susceptibility of the mononuclear compound Cp^*RuCl_2(pyridine) (**4**); (iii) the EPR spectra of magnetically diluted samples of Cp^*RuCl_2 in $[Cp^*Rh(\mu\text{-}Cl)Cl]_2$ (**5**) (Rh−Rh = 3.72 Å [9]) and $[Cp^*Ir(\mu\text{-}Cl)Cl]_2$ (**6**) (Ir−Ir ≈ 3.77 Å [10]), which can be expected to contain Ru dimers nearly identical to isomer **1b**. The molecular structures and spin states of the binuclear compounds are discussed in the framework of the extended Hückel model.

Experimental Section

Magnetic Susceptibility Measurements. Variable temperature (3−295 K) magnetic susceptibility measurements on powdered samples (5−13 mg) of **1**−**4** (starting material: $RuCl_3$ hydrate; purity 99.9%; Johnson-Matthey, Reading, England) have been carried out using a Faraday balance with $HgCo(NCS)_4$ [11] as standard at magnetic fields between 0.1 and 1.4 T. High purity samples of **1**−**3** have been obtained from suitable single crystals which were checked for lattice parameters on a diffractometer. The susceptibilities which have been found to be independent of the magnetic field strength were corrected for the diamagnetism of the molecular systems (-232 × 10^{-11} (**1**), −248 × 10^{-11} (**2**), −265 × 10^{-11} (**3**), and −313 × 10^{-11} (**4**) $m^3\ mol^{-1}$/Ru; SI units[12]). Figure 2 exhibits the temperature dependence of the effective Bohr magneton numbers n_{eff} of **1** and **4**, the former referring to *two* metal centers and the latter to *one* center. In Figure 3 the $\chi-T$ plots of **2** and **3** are presented.

EPR Measurements. Magnetically diluted samples of Cp^*RuCl_2 in $[Cp^*Rh(\mu\text{-}Cl)Cl]_2$ (**5**) and $[Cp^*Ir(\mu\text{-}Cl)Cl]_2$ (**6**) respectively were prepared by dissolving the complexes in the appropriate proportion in CH_2Cl_2 and rapidly evaporating the solvent in vacuo. The purity of the samples was checked by X-ray powder diffraction[13] (Guinier method). X-band spectra of the resulting crystalline powders were recorded at 5−10 K at 9127 MHz microwave frequency on a Varian E6 EPR spectrometer equipped with a RMN2 gaussmeter. A representative EPR spectrum of 11% Cp^*RuCl_2 doped into **5** is shown in Figure 4.

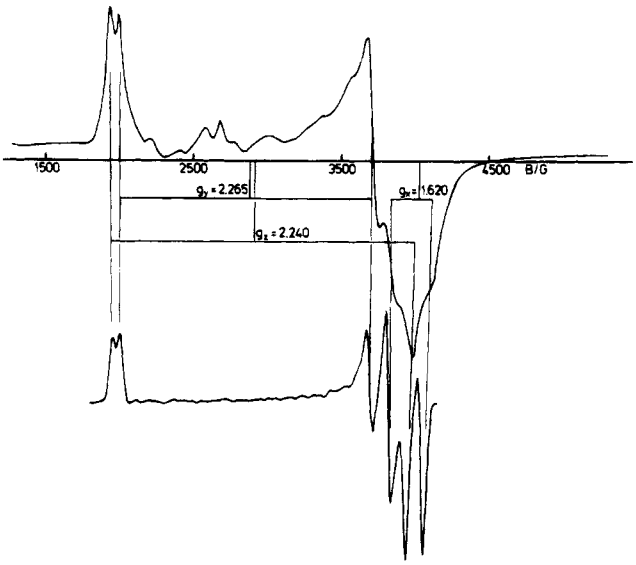

Figure 4. EPR spectrum of 11% Cp^*RuCl_2 doped into **5** and simulation.

Results

Magnetic Properties. Cp^*RuCl_2(py) (4, py = pyridine). This compound, serving as a reference for organo-metallic Cp^*Ru^{III} low-spin complexes with an isolated Ru center, exhibits Curie paramagnetism. The effective Bohr magneton number n_{eff} varies slightly from 2.0 to 1.9 between 295 and 7 K (see Figure 2), confirming that the paramagnetic centers have low-spin configuration. The magnetic behavior in this temperature range can be approximated by $n_{eff} = g[S(S+1)]^{1/2}$ with $S = {}^1/_2$ and $g \approx 2.3$. Below 7 K n_{eff} decreases more rapidly, finally reaching 1.7 at 3.3 K. The overall behavior is similar to the magnetism of other mononuclear Ru(III) coordination complexes, reflecting the combined effect of the ligand field and spin−orbit coupling.

$[Cp'Ru(\mu\text{-}Cl)Cl]_2$ (2) and $[Cp^*Ru(\mu\text{-}Br)Br]_2$ (3). The two complexes which form dimers similar to molecule **1a** (see Table 1) are very weakly paramagnetic in the order of the diamagnetic correction; e.g., $\chi \approx (200 \pm 40) \times 10^{-11}$ $m^3\ mol^{-1}$/Ru at 295 K for **3** (see Figure 3), a finding which indicates relatively strong antiferromagnetic spin coupling of the $S_1 = S_2 = {}^1/_2$ centers. The increase of χ with decreasing temperature is presumably due to Curie paramagnetic impurities which are present in a small amount in the crystalline material. A slight increase of the susceptibility data with increasing temperature is observed

(9) Churchill, M. R.; Julis, S. A.; Rotella, F. J. *Inorg. Chem.* **1977**, *16*, 1137.
(10) Churchill, M. R.; Julis, S. A. *Inorg. Chem.* **1977**, *16*, 1488.
(11) Nelson, D.; ter Haar, L. W. *Inorg. Chem.* **1993**, *32*, 182.
(12) Weiss, A.; Witte, H. *Magnetochemie-Grundlagen und Anwendungen*; Verlag Chemie: Weinheim, Germany, 1973.
(13) Lattice parameters of the mixed metal compounds have been refined and found to be close to the parameters of **5** and **6** (space group $P2_1/c$ [9,10]). In the case of **5** doped with 11% Cp^*RuCl_2 the lattice constants are a = 8.370(4) Å, b = 9.193(3) Å, c = 15.677(9) Å, β = 106.77-(6)° (lattice parameters of **5** for comparison: a = 8.375(1) Å, b = 9.228(2) Å, c = 15.651(2) Å, β = 106.70(1)° [9]).

in the case of **2** above 150 K, a behavior that can in principle be related to the beginning occupation of the excited triplet state, suggesting a weaker antiferromagnetic coupling in **2** than in **3**.

The magnetic behavior of **2** and **3** has been analyzed with the Bleaney–Bowers formula[14] for an isotropically exchange coupled $S_1 = S_2 = {}^1/_2$ system (exchange operator $\hat{H} = -2J_a\hat{S}_1\cdot\hat{S}_2$; J_a, exchange parameter) corrected for temperature dependent and temperature independent contributions,

$$\chi = (1 - \delta)\chi(\mathbf{a}) + \delta C/T + \chi_0 \qquad (1)$$

with

$$\chi(\mathbf{a}) = \frac{\mu_0 N \mu_B{}^2}{3kT} \frac{g_a{}^2}{1 + (1/3)\exp(-2J_a/kT)} \qquad (2)$$

where $\chi(\mathbf{a})$ refers to one metal center of an **a** dimer. The quantities μ_0, N, g_a, μ_B, k, and C are vacuum permeability, Avogadro number, g factor, Bohr magneton, and Boltzmann and Curie constants, respectively, while δ represents the fraction of a monomer impurity.

Taking $g_a = 2.3$ from the experimental data of **4** and C for a mononuclear Ru(III) low-spin complex, the exchange parameter values $-J_a = 380 \pm 40$ cm^{-1} (**2**) and ≥ 450 cm^{-1} (**3**) are obtained (quality factor SQ = 3–5% [15]). The error given for **2** contains the accuracy of the measurements and the correlation with other parameters, e.g., χ_0. For **3** an increase of $|J_a|$ above the quoted value did not produce any improvement. With choice of an appropriate C for a $S = {}^1/_2$ impurity, δ is in the range 0.07–0.09 and χ_0 yields only a small negative correction for **2** ($-(40 \pm 40) \times 10^{-11}$ m^3 mol^{-1}) and a positive one for **3** ($(80 \pm 40) \times 10^{-11}$ m^3 mol^{-1}). Using C corresponding to a $S = {}^5/_2$ species produces δ values in the range 0.005–0.008 but hardly changes the value of J_a (2%). The same is true for a variation of g_a within reasonable limits ($\Delta g_a = \pm 0.2$). The solid and broken lines in Figure 3 correspond to fits with g_a and C fixed to 2.3 and 5.5×10^{-5} m^3 K mol^{-1}, respectively, and δ, $-J_a$, and χ_0 refined to 0.0083 (0.0054), 380 (500) cm^{-1}, and -70×10^{-11} (100×10^{-11}) m^3 mol^{-1} for **2** (**3**). Due to competing diamagnetic and paramagnetic contributions, the measured mass susceptibilities are extremely small. To obtain more exact information about the energy separation between the singlet and the excited triplet state,[16] susceptibility measurements had to be extended above room temperature, which is precluded by the thermal instability of the compounds.

To summarize, the simulations yield negative J_a values at least of the order 400 cm^{-1} for the intramolecular antiferromagnetic coupling of the Ru spins, as has been observed for, e.g., sulfur bridged dimeric ruthenium complexes.[17,18]

$[Cp^*Ru(\mu\text{-}Cl)Cl]_2$ (1). In contrast to **2** and **3** complex **1** consists of the two types of dimers **1a** and **1b** (ratio 1:1) and shows a more complicated behavior: (i) the χ^{-1}–T plot is curved and cannot therefore satisfactorily be approximated by a Curie–Weiss law; (ii) a susceptibility maximum is found at 6 K; (iii) in the temperature range from 295 to 60 K n_{eff} *per metal atom* is roughly $1/\sqrt{2}$ times smaller than that of the mononuclear complex ($n_{eff} \approx 1.5$ and 2.0, respectively). Obviously, only half the metal centers are Curie paramagnetic. This agrees with the results from NMR experiments,[8] which have been interpreted on the basis of paramagnetic (**1b**) and diamagnetic (**1a**) binuclear units, the latter with singlet ground state ($S = 0$) due to intramolecular antiferromagnetic spin coupling just as in **2** and **3**. In the temperature range from 60 to 8 K n_{eff} increases slightly with decreasing temperature. Hence, it appears that in molecule **1b** Ru spins are weakly *ferromagnetically* coupled (spin triplet ground state $S = 1$). At 8 K n_{eff} reaches a maximum and subsequently decreases rapidly (see Figure 2). This behavior is traced back to intermolecular antiferromagnetic ordering of the $S = 1$ spins of dimers **1b** (intermolecular Ru(**1b**)–Ru(**1b**) distance: 7.925 Å).

The data above the susceptibility maximum ($T \geq 6$ K) have been analyzed in terms of the isotropic Heisenberg model. In this model the susceptibility for an ensemble of dimers **1a** and **1b**, allowing for Curie paramagnetic and temperature independent correction, is expressed as

$$\chi = (1 - \delta)[\chi(\mathbf{1a}) + \chi(\mathbf{1b})] + 2\delta C/T + \chi_0 \qquad (3)$$

where $\chi(\mathbf{1a})$ and $\chi(\mathbf{1b})$ refer to Bleaney–Bowers expressions with parameters g_a, J_a, and g_b, J_b, respectively.

In the fitting procedures g_a and J_a have been taken from **2** in view of the close resemblance in molecular structures and the bridge atoms. Assuming a monomer fraction $\delta = 0.0083$ ($C = 5.5 \times 10^{-5}$ m^3 K mol^{-1}), the refinement of g_b, J_b, and χ_0 yields the parameter values $g_b = 2.40$, $J_b = 11.9$ cm^{-1}, and $\chi_0 = -227 \times 10^{-11}$ m^3 mol^{-1} (SQ = 2.1%). This result is presented in Figure 2 (solid line). The parameters δ, g_b, and χ_0 are strongly correlated. If, on the one side, the monomer contribution is neglected, the parameter values $g_b = 2.52$, $\chi_0 = -100 \times 10^{-11}$ m^3 mol^{-1}, and $J_b = 12.0$ cm^{-1} are obtained (SQ = 1.9%). On the other side, if g_b is fixed to 2.3, the values $\delta = 0.015$, $\chi_0 = -284 \times 10^{-11}$ m^3 mol^{-1}, and $J_b = 11.6$ cm^{-1} (SQ = 2.4%) ensue, i.e., the adjusted J_b value is nearly independent of a paramagnetic impurity of the expected order of magnitude. In final calculations on the basis of eq 3 the influence of varying J_a has been considered. With $|J_a| < 400$ cm^{-1} the fit is less satisfactory, whereas a variation of the exchange parameter toward a higher singlet–triplet splitting does not produce any improvement.

The fit is hardly improved (SQ = 1.5%) allowing for magnetic interactions between triplet dimers **1b** in the molecular field approximation (replacing $\chi(\mathbf{1b})$ in eq 3 by $\chi(\mathbf{1b})' = \chi(\mathbf{1b})/[1 - \lambda\chi(\mathbf{1b})]$ with a small positive molecular field parameter λ corresponding to $\Theta_p = 0.7$ K, but nearly identical g_b and J_b. With regard to the behavior of **1** below 8 K the effect of zero-field splitting within the triplet ground state has been investigated. $\chi(\mathbf{1b})$ in eq 3 was extended by second-degree crystal field terms with orthorhombic symmetry using the pair Hamiltonian[19]

$$\hat{H} = -2J_b\hat{S}_1\cdot\hat{S}_2 + D_e(3\hat{S}_{1z}\hat{S}_{2z} - \hat{S}_1\cdot\hat{S}_2) + E_e(\hat{S}_{1x}\hat{S}_{2x} - \hat{S}_{1y}\hat{S}_{2y}) \qquad (4)$$

The powder susceptibility is given by $\chi = (\chi_x + \chi_y + \chi_z)/3$ with g_x, g_y, and g_z respectively replacing the isotropic parameter

(14) Bleaney, B.; Bowers, K. D. *Proc. R. Soc. London, Ser. A* **1952**, *214*, 451.

(15) SQ = $(FQ/n)^{1/2}$ with FQ = $\sum_{i=1}^{n}[\{\chi_o(i) - \chi_c(i)\}/\chi_o(i)]^2$ (n = number of measured values; χ_o and χ_c measured and calculated susceptibility data, respectively).

(16) From the temperature dependent equilibrium **1a** ⇌ **1b** in solution an enthalpy difference $\Delta H_R \approx 15$ kJ mol^{-1} (1250 cm^{-1}) was estimated (see ref 4). If it is assumed that only one paramagnetic form, i.e., **1b**, is present in solution, then the singlet–triplet separation of **1a** must be higher in energy than ≈1250 cm^{-1}.

(17) Dev, S.; Imagawa, K.; Mizobe, Y.; Chang, G.; Wakatsuki, Y.; Yamazaki, H.; Hidai, M. *Organometallics* **1989**, *8*, 1232. Dev, S.; Mizobe, Y.; Hidai, M. *Inorg. Chem.* **1990**, *29*, 4797.

(18) Rauchfuss, T. B.; Rodgers, D. P. S.; Wilson, S. R. *J. Am. Chem. Soc.* **1986**, *108*, 3114.

(19) Owen, J.; Harris, E. A. In *Electron paramagnetic resonance*; Geschwind, S., Ed.; Plenum Press: New York, London, 1972; Chapter 6, p 427.

g_b. Calculations using realistic values for D_e and E_e and varying anisotropic g values show that the experimental maximum in n_{eff} cannot be reproduced by the model. Instead a constant value at low temperature is obtained. Hence, the magnetic behavior below 8 K cannot be explained by anisotropic spin−spin coupling but must be due to intermolecular antiferromagnetic ordering.

EPR Measurements. Cp*RuCl$_2$(py) (4). A powder spectrum of **4**, diluted in the rhodium analogue, exhibits relatively narrow lines (40 G) with g values 2.84, 2.01, and 1.87 (mean value 2.24, close to $g = 2.3$ deduced from the susceptibility measurement).

[Cp*Rh(μ-Cl)Cl]$_2$ (5) and [Cp*Ir(μ-Cl)Cl]$_2$ (6) Doped with Cp*RuCl$_2$. The EPR spectra of frozen solutions of Cp*RuCl$_2$ in CH_2Cl_2 are featureless and of low intensity. This is due to the rapid equilibrium **1a** ⇌ **1b** in solution with **1a** prevailing at low temperature. A frozen solution therefore consists of mostly **1a**, which is EPR silent. Neither room temperature spectra in solution nor undiluted solid samples give any information.

In order to obtain a better resolved spectrum of **1b** at low temperature, Cp*RuCl$_2$ has been magnetically diluted into the rhodium (**5**) and iridium (**6**) analogues, known to have the same structure with metal−metal distances close to the one found for **1b** (Ru−Ru = 3.75 Å[4]; Rh−Rh = 3.72 Å[9]; Ir−Ir = 3.77 Å[10]). Room temperature NMR spectra in CD_2Cl_2 of a 1:10 mixture of Cp*RuCl$_2$ in **5** display a sharp signal at 1.56 ppm which is assigned to the Cp* ligand of **5**. At high proportions of the ruthenium complex (≈30%) appears a broad absorption around 7 ppm, characteristic for the equilibrium **1a** ⇌ **1b** along with a second broad signal near 1.5 ppm which has been assigned to the Cp*Rh part in the mixed metal complex [Cp*RhCl(μ-Cl)$_2$RuClCp*]. This observation proves slow redistribution on the NMR time scale with predominantly homometallic species present at low Ru concentration.

EPR powder spectra of Cp*RuCl$_2$ magnetically diluted in **5** (2, 5, 8, 11, and 15 at. %) and in **6** (10 at. %) are in close resemblance and consist of a basic six-line pattern with two lines near 1950 G and four around 3800 G. Additional weak signals are observed around ≈1500 and 2640 G and in the high-field portion of the spectrum (see EPR spectrum of sample **5** (11%), Figure 4), the latter increase in intensity with increasing Ru proportion. The nearly identical spectra in the Rh ($I = {}^1/_2$) and Ir ($I = {}^3/_2$) host lattices rule out hyperfine coupling within the mixed metal dimer as the origin of the six-line spectrum. This is therefore assigned to the triplet state of the Ru−Ru dimer **1b** fixed in the geometry of the respective host lattice. On account of the triplet−singlet splitting of ≈24 cm^{-1}, determined from magnetochemical analysis of **1**, transitions between the states $S = 0$ and $S = 1$ cannot be observed. The $\Delta M = 2$ transition within the triplet must be of low intensity and could not be identified among other small spurious signals around 1500 G. Furthermore, no significant change in intensity of the EPR spectrum has been noted by decreasing the temperature from 10 to 5 K, which result can be expected with regard to the magnitude of the triplet−singlet splitting.

As the exchange interaction is much greater than the expected zero-field splitting, the system can be described in terms of the total spin S. The spectrum has been simulated fitting g values and zero-field splitting parameters D and E using the program MAGRES[20] (see Figure 4). A fit compatible with the condition $|D| \geq 3|E|$, showing a small discrepancy of observed and calculated line position in the high field z component, is obtained for the parameter set $g_x = 1.620$, $g_y = 2.265$, $g_z = 2.240$, $D = 0.0976$ cm^{-1}, and $E = 0.0266$ cm^{-1}. The weaker signals at $g = 2.5$ and 2.0 probably originate in the mixed metal species.

The EPR powder spectra manifest the spin triplet ground state of dimer **1b** and hence confirm the weak ferromagnetic spin coupling detected by the susceptibility measurement of **1**.

Conclusion

In conclusion, the spin couplings between the Ru(III) low-spin centers in the two isomers of **1** differ distinctly owing to the geometry of the halide bridge and the Ru−Ru distance. In molecule **1a**, an antiparallel coupling of the Ru spins is observed with a singlet−triplet splitting of at least $|2J| \approx 760$ cm^{-1} as a consequence of the short Ru−Ru separation (2.93 Å) and the small bridge angle (76°). In molecule **1b**, however, a weak ferromagnetic coupling of the Ru spins occurs (triplet−singlet splitting ≈ 24 cm^{-1}), obviously controlled by superexchange effects via the chlorine bridge on account of a favorable bridge angle of 100° and the absence of direct exchange interaction (Ru−Ru = 3.75 Å).

Electronic Structure

The outstanding structural feature of **1** with the coexistence of two "deformational" isomers **1a** and **1b** and their magneto-structural correlation calls for an explanation on the basis of molecular orbital ideas. The change in spin state with Ru−Ru distance and Ru−Cl−Ru angle is reminiscent of related phenomena in Cu(II) dimers,[21] where the Cu(II) units are one electron short of a filled σ (e_g descendent) shell and the Cp*RuX$_2$ monomeric moiety with a d^5 low-spin configuration is one electron short of a filled π (t_{2g} descendent) shell. In the copper systems the effect of the Cu−bridge−Cu angle on the exchange interaction has been studied extensively. Antiferromagnetically coupled spins are observed with bond angles larger than ≈100°, and systems with smaller angles (97−95°) have ferromagnetically coupled spins. Hay et al.,[22] whose model shall profitably be recalled here, have derived the expression

$$E_S - E_T = 2K_{ab} - 2(\epsilon_1 - \epsilon_2)^2/(J_{aa} - J_{ab})$$

for the singlet−triplet splitting and have analyzed the observed angular dependence of this energy difference in the framework of extended Hückel theory using the HOMO−LUMO gap $\epsilon_1 - \epsilon_2$ as the dominant factor in antiferromagnetic interactions. As the bridge angle decreases in size, the HOMO−LUMO gap for the singlet (antiferromagnetic) configuration decreases in magnitude. At a critical value the balance between the one-electron forces (crudely the HOMO−LUMO gap of the one-electron model) and the two-electron exchange interaction K_{ab} is such that the triplet (ferromagnetic) arrangement is more stable. On further reduction of the angle (<95°), the model predicts again a singlet ground state on account of an increasing HOMO−LUMO gap and direct metal−metal interaction. Since the two-electron terms (exchange interaction K_{ab}, Coulomb interactions J_{aa}, J_{ab}) seemed to vary little with angle, these authors were able to identify the variation of the HOMO−LUMO gap with the Cu−bridge−Cu angle as the crucial part of the problem and to produce an explanation of this variation by a study of the atomic orbital composition of the two relevant molecular orbitals. We shall follow a similar course here using the extended Hückel model to explain the findings concerning structure and magnetism of the ruthenium compounds. We

(20) Keijzers, C. P.; Reijerse, E. J.; Stam, P.; Dumont, M. F.; Gribnau, M. C. M. *J. Chem. Soc., Faraday Trans. 1* **1987**, *83*, 3493.

(21) Willett, R. D. Ref 2, p 389.

(22) Hay, P. J.; Thibeault, J. C.; Hoffmann, R. *J. Am. Chem. Soc.* **1975**, *97*, 4884.

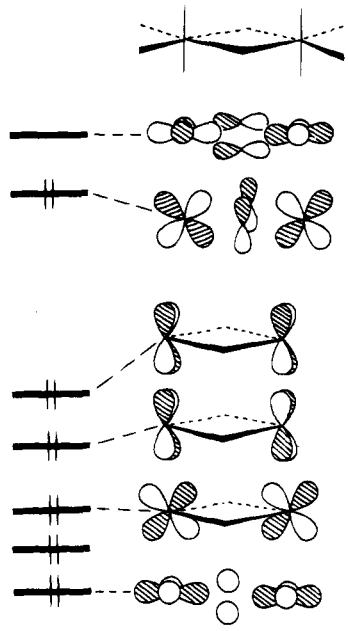

Figure 5. Approximate orbital composition of the t_{2g} blocks for the antiferromagnetic chloride with a bridge angle of 81° (see text).

should realize, however, that the isomorphism with the copper dimers is not exact since the form of the orbitals is different.

In Figure 5 is depicted the approximate orbital composition of the t_{2g} blocks of the orbitals for a structure with the bond lengths appropriate for the antiferromagnetic chloride and a bridge angle of 81°. (One orbital, left unmarked, is a largely chlorine located orbital.)

Figure 6 shows the calculated energy levels in the frontier-orbital region for the one bromo (**3**) and the two isomers of the chloro complex (**1a**, **1b**). For simplicity we have replaced the Cp* ligand with Cp, but otherwise the geometries are exactly those of the crystal structure.[4] The HOMO of the respective singlet configurations is indicated with an arrow. Notice that the collection of energy levels found for these species is qualitatively in accord with their observed magnetic properties, for the two singlet (antiferromagnetic) species have significantly larger HOMO−LUMO gaps than the triplet (ferromagnetic) example. In the case of the triplet chloro complex there are a number of energy levels close to that of the HOMO of the singlet configuration but perhaps too high in energy to allow more than one unpaired electron per metal atom, i.e., to destabilize the d^5 low-spin configuration.

In order to probe the influence of the geometry on the atomic orbital interaction in more detail, we have studied the orbital structure of $[H_3RuCl(\mu\text{-}Cl)_2ClRuH_3]^{4-}$ (**7**) as a model system

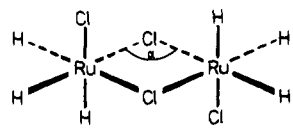

7

as a function of the Ru−Cl−Ru bridge angle, where the Cp ligand is mimicked by a trio of hydrogen atoms. This simplification will in fact capture the essence of the electronic situation. The substitution should allow for a closer insight into the orbital overlap variation when the molecular geometry is varied. In view of the change in energy and also in orbital composition brought about by the change of Cp for 3H + 2e the results of this analysis can have only a qualitative impact on the real electronic situation. The atomic orbital energies for Cl 3p and Ru 4d are close,[23] and the "dπ region" of the molecule

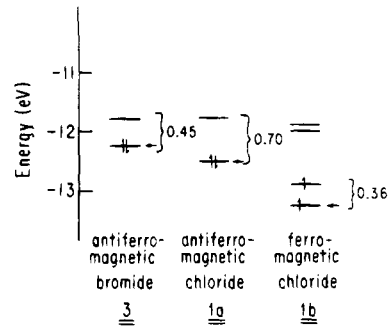

Figure 6. Calculated energy levels of **3**, **1a**, and **1b** in the frontier-orbital region.

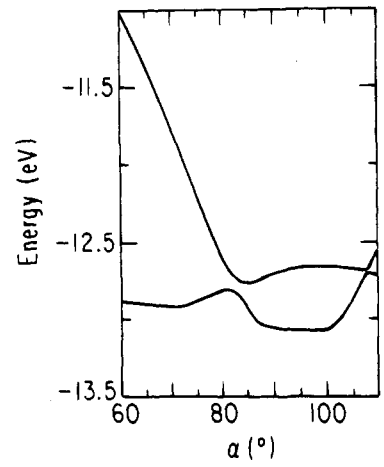

Figure 7. Variation of the HOMO and LUMO orbital energies as a function of the Ru−Cl−Ru bridge angle α calculated for the model system **7**.

contains both bonding and antibonding Ru−Cl orbitals in addition to chlorine lone pairs. The two highest energy orbitals of the set lie a little above the rest for a wide range of geometries. These are the HOMO and LUMO of the singlet configuration depicted in **7a** and **7b** for a Ru−Cl−Ru angle of 80°.

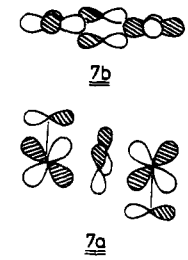

7b

7a

In Figure 7 the variation of the HOMO and LUMO orbital energies is presented, and Figure 8 shows the variation of the HOMO−LUMO gap with Ru−Cl−Ru bond angle α. The results are readily understood in terms of overlap arguments. When α = 90°, orbital **7b** is involved purely in π-type interaction with the metal, but as this angle either opens or closes, a Ru−Cl σ-antibonding interaction is switched on and this orbital is destabilized. One minimum in the energy of this orbital is thus expected at around 90°. The metal−ligand π overlap, which determines the energy of orbital **7a**, has a maximum at α = 180° (it varies as sin[α/2]).[24] Thus, in the α

(23) EH parameters (exponents, H_{ii} (eV)): Ru 5s, 2.08, −10.44; Ru 5p, 2.04, −6.87; Ru 4d, 5.38 (0.5342), 2.30 (0.6368), −14.9. The d orbital parameters are double ζ ones with coefficients in parentheses. The Ru−H distance is 1.9 Å.

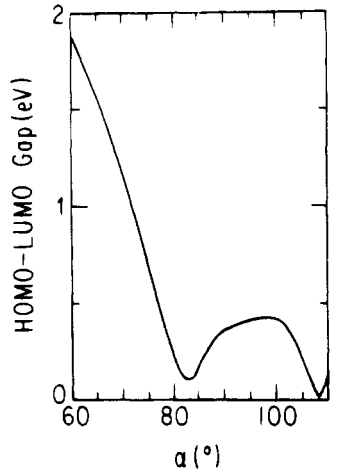

Figure 8. Variation of the HOMO−LUMO gap as a function of α calculated for **7**.

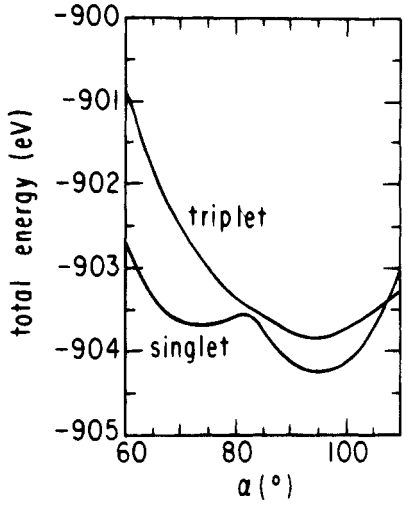

Figure 9. Variation of the total energy of the singlet and triplet isomers as a function of α calculated for **7**.

range of interest, the energy of this orbital increases as α increases. An important orbital crossing (actually an avoided crossing given the molecular symmetry) occurs close to 83°, which complicates the picture slightly.

Figure 9 shows the total energetic variation of the singlet and triplet isomers as a function of α obtained after adding the contribution of the $[Kr]4d^4-[Kr]4d^4$ core to the plot of Figure 7. The latter decreases with increasing α and probably just represents relief of steric repulsion, significant at small values of α. The triplet isomer has one energy minimum at 95° close to the angle of 100° found experimentally in the structure of **1b**. The singlet isomer has two minima, one at around 95° and the other at the lower angle of 74°. The latter is close to the experimentally observed geometry of 76° in the structure of **1a**. The location of these calculated minima are readily understood from the variation in energy of the HOMO and LUMO (see above). Hence, the origin of the minima in the plots of Figure 9 are easy to see: Those at the higher value of α for both triplet and singlet situations is set by minimizing the Ru−Cl σ-antibonding interaction in orbital **7b**. The lower angle minimum for the singlet configuration is set by the balance between the steric interactions and π-antibonding interactions, the former decreasing and the latter increasing as α increases. Notice that there is a barrier between the two singlet minima. Whereas the singlet configuration is stable at the lower angle minimum due to the large energy separation to the triplet at this geometry, it is obviously unstable at the higher angle minimum. Here the singlet−triplet separation is much less and could be easily overcome by the gain in spin-pairing energy, making the triplet the ground state. In view of the qualitative nature of our one-electron model we cannot, of course, comment on the true singlet−triplet energy separation. However, an antiferromagnetic situation with a small value of α and a ferromagnetic one with a larger value of α are a natural result of the molecular orbital structure.

There is also a significant change in Ru−Cl bond length on moving from one isomer to another, which is readily appreciated from the form of the orbitals **7a** and **7b**. Indeed, we can see that the HOMO of the singlet form at the low-angle minimum (orbital **7a**) is Ru−Cl_T π-antibonding but only weakly (at least at small α values) Ru−Cl_B π-antibonding. The LUMO (orbital **7b**) is Ru−Cl_T nonbonding but is Ru−Cl_B π-antibonding. Thus on moving from the singlet to triplet form a Ru−Cl_T π-antibonding electron is converted into a Ru−Cl_B π-antibonding electron. As a result the terminal Ru−Cl distances shorten (from 2.418 to 2.365 Å) and the bridging one lengthens (from 2.366 to 2.432 Å) on going from the singlet to the triplet isomer.

HOMO−LUMO separation and orbital occupancy as derived from extended Hückel model calculations give a consistent picture for the spin states and the magnetic interactions found in the two "deformational" isomers **1a** and **1b** of $[Cp^*Ru(\mu\text{-}Cl)Cl]_2$. The similarity to Cu(II)−Cu(II) systems alluded to above is obvious. The M−bridge−M geometry in the triplet dimer **1b** (α = 100°) corresponds to the ferromagnetically coupled binuclear Cu(II) species with α ≈ 96°. The copper analogue to the singlet dimer **1a** has been predicted[22] but not yet observed experimentally.

For smaller angles α and corresponding metal−metal distances < 3 Å the question of direct metal−metal versus through-ligand interactions arises. Clearly the direct metal−metal interactions increase as α decreases. However, although the HOMO−LUMO gap increases for smaller α, we cannot separate in our calculations the effect of the direct, out-of-phase, metal−metal interaction in the LUMO from that associated with the through-bond coupling. We do note that on the simplest model possible, using the angular overlap approach and ignoring metal−metal interactions, the HOMO−LUMO crossing should occur at 90°.

The structural dichotomy found in $[Cp^*RuCl_2]_2$ is expected to occur in other binuclear complexes, where direct metal−metal bonding and ligand−ligand repulsion counterbalances. The simultaneous existence of both forms in the crystal structure is highly fortuitous and requires among other things a favorable packing in the solid state.

Acknowledgment. We are most indebted to Dr. E. J. Reijerse, Faculty of Science, University of Nijmegen, for having set a PC version of the program MAGRES at our disposal and for his kind help in getting started. Our thanks are due to Prof. Dr. D. Reinen, Fachbereich Chemie der Philipps-Universität Marburg, for a helpful discussion and Dipl.-Phys. U. Weber, II. Physikalisches Institut, TH Aachen, for assisting in the EPR measurements. Financial support by Deutsche Forschungsgemeinschaft and Fonds der Chemischen Industrie is gratefully acknowledged. Johnson-Matthey Co., Reading, England, is thanked for a loan of $RuCl_3$. S.B. was supported by the REU Program at the University of Chicago.

IC950637X

(24) See, for example: Burdett, J. K. *Molecular Shapes*; Wiley: New York, 1980.